Decadal Variability in the Arctic Ocean – Greenland-Iceland-Norwegian Seas Ice-Ocean-Atmosphere Climate System

Dmitry Dukhovskoy[*], Mark Johnson[**], Andrey Proshutinsky[***]

[*] Institute of Marine Science, University of Alaska Fairbanks, Fairbanks, Alaska, USA; currently at Center for Ocean-Atmospheric Prediction Studies, Florida State University, Tallahassee, Florida, USA; ddmitry@coaps.fsu.edu.
[**] Institute of Marine Science, University of Alaska Fairbanks, Fairbanks, Alaska, USA; johnson@ims.uaf.edu.
[***] Physical Oceanography Department, Woods Hole Oceanographic Institution, Woods Hole, Massachusetts, USA; aproshutinsky@whoi.edu.

Recent studies suggested decadal time scale as the most dominant of the Arctic climate variability [e.g., *Mysak and Venegas*, 1998]. The origin of the Arctic climate decadal variability and mechanisms regulating this variability are still unclear and need to be determined and investigated. In this study we generalize and investigate in detail a mechanism of decadal variability in the Arctic proposed by *Proshutinsky and Johnson* [1997] and *Proshutinsky et al.* [2002].

The Arctic Ocean and the GIN Sea (Greenland, Iceland, Norwegian Seas) are viewed as a closed ice-ocean-atmosphere climate system. Decadal variability in this system is driven by fresh water (FW) and sensible heat fluxes controlled by alternating between-basin oceanic and atmospheric gradients. When the Arctic High prevails (anticyclonic circulation regime (ACCR) or low AO/NAO), the interaction between basins is suppressed and the fluxes are weak. When the Icelandic Low prevails (cyclonic circulation regime (CCR) or high AO/NAO), the interaction between the basins is intense and the fluxes are strong. The hypothesized behavior of the system is shown on Fig. 1.

An idealized Arctic Ocean – Greenland Sea model has been designed (Fig. 2) to reproduce the cyclic anticyclonic/cyclonic (low/high AO or NAO) regime shift in the Arctic Ocean as an auto-oscillatory behavior of the studied region. The Arctic module includes an Arctic Ocean model coupled to a thermodynamic sea ice model, a sea-ice shelf model, and an atmospheric box model. The Arctic Ocean model is one-dimensional, three-layer and time-dependent similar to *Björk* [1989]. The atmospheric box model estimates SAT from the total energy balance, with interannual variability induced by varying heat flux, F_h, from the Greenland Sea atmospheric box. F_h is a function of surface air temperature (SAT) difference between the Arctic and the Greenland Sea modules. The Greenland Sea ocean model is one-dimensional and time dependent and is, in general, similar to the Arctic Ocean model. The oceanic model is coupled to a thermodynamic sea ice model and an atmospheric model. The atmospheric model calculates SAT anomalies for computed surface heat flux. The Greenland Sea module describes the seasonal and interannual variability of the heat content of the GIN Sea region assuming that it is related to the air-sea surface heat flux. The air-sea heat flux, in turn, is determined by the intensity of deep convection in the Greenland gyre which is controlled by the amount of FW advected from the Arctic Ocean (F_{fw}). The model has been run for 110 years, with the first 10 years spin-up. Different climate states are reproduced in the model by different rates of F_{fw} and F_h (Figs. 3a and 3b).

The major result of the study is that the model reproduces the hypothesized behavior of the system (compare Fig. 3c with Fig. 1). The period of simulated oscillations is 10 to 15 years (Fig. 3d) which agrees with *Proshutinsky and Johnson* [1997]. To demonstrate the correspondence of the model output to observations, simulated and observed SAT and net surface heat flux in the Arctic and Greenland Sea are presented in Fig. 4. Note the difference between the characteristics simulated for different regimes (blue and red curves).

Acknowledgments. This research has been supported by the National Science Foundation and by the International Arctic Research Center, University of Alaska Fairbanks, under auspices of the United States National Science Foundation and from the Alaska Sea Grant through the Center for Global Change, University of Alaska Fairbanks.

References

Björk, G., A one-dimensional time-dependent model for the vertical stratification of the upper Arctic Ocean, J. Phys. Oceanogr., 19, 52 - 67, 1989.

Mysak, L.A., and S.A. Venegas, Decadal climate oscillations in the Arctic: A new feedback loop for atmospheric-ice-ocean interactions, *Geophys. Res. Lett.*, *25* (19), 3607-3610, 1998.

Proshutinsky, A.Y., and M.A. Johnson, Two circulation regimes of the wind-driven Arctic Ocean, *J. Geophys. Res.*, *102*, 12493 - 12514, 1997.

Proshutinsky, A., R.H. Bourke, and F.A. McLaughlin, The role of the Beaufort Gyre in Arctic climate variability: Seasonal to decadal climate scales, Geophys. Res. Lett., 29 (23), 2100, doi: 10.1029/2002GL015847, 2002.

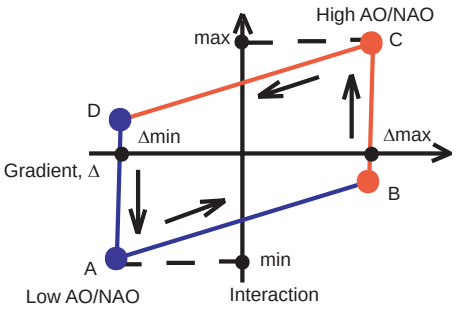

Fig. 1. Hypothesized behavior of the Arctic – GIN Sea climate system. Abscissa is the between-basin gradient of SAT or dynamic height. Ordinate is the intensity of interaction between the basins, either FW or heat flux. Blue segments denote weak interaction and red segments intense interaction.

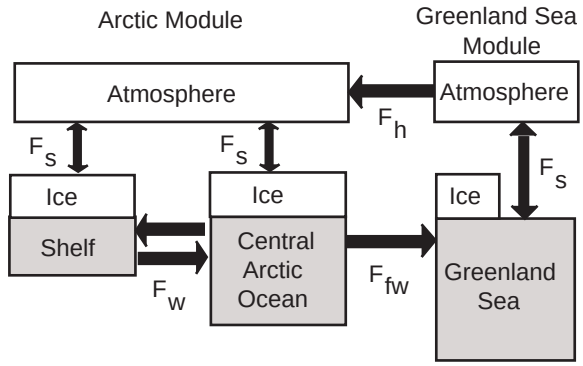

Fig. 2. Schematic of the Arctic Ocean – Greenland Sea model system. F_s is surface heat flux, Fw is water exchange between the Arctic Ocean model and Arctic shelf box model, F_{fw} is the freshwater flux to the Greenland Sea model, F_h is heat flux to the Arctic atmospheric model.

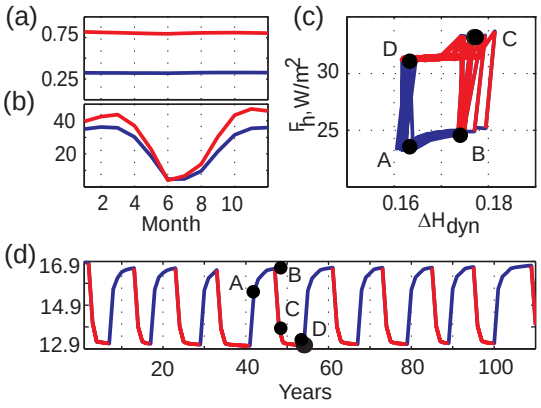

Fig. 3. (a) Monthly freshwater outflow from the upper 100 m of the Arctic Ocean during the weak interaction phase (blue) and strong interaction phase (red). (b) Similar to (a) but for the heat flux. (c) Heat flux vs. gradient of dynamic height (ΔH_{dyn}) for 110 years of simulated behavior (compare with Fig. 1). (d) Annually averaged SAT gradient (ΔT) for 110 years. Bullets denote system states shown on (c). On (c) and (d), red segments denote high AO/NAO years, blue low AO/NAO.

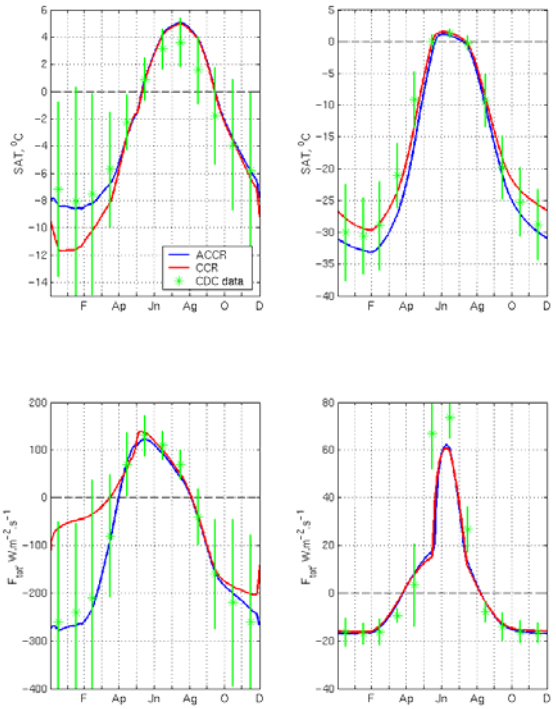

Fig. 4. Model output: Mean ACCR and CCR SAT and surface heat flux in the Arctic Ocean and Greenland Sea. Time series of simulated daily SAT in the Greenland Sea (a) and the Arctic Ocean (b) averaged over the last years of ACCR (blue lines) and CCR (red lines) forcing. Green asterisks denote monthly mean values obtained from NOAA-CIRES CDC data over the period 1948-2001. Vertical green bars are the 98% confidence intervals for the CDC means. Abscissa is time, end of months. (c) Same as (a) but for the Greenland Sea surface heat flux. (d) Same as (b) but for the Arctic Ocean surface heat flux.

Study of Air-Sea Interaction over Hudson Bay and its Effect on Regional Climate of Québec by using the MRCC coupled with MRO.

Minwei QIAN[(1)], Daniel CAYA[(2)], François SAUCIER[(3)] and René LAPRISE[(1)]

(1) Université du Québec à Montréal
(2) Ouranos
(3) Institut Maurice-Lamontagne de Pêches et Océans Canada

Abstract

The MRCC (Modèle Régional Canadien du Climat), which is developed at UQAM, has been coupled with MRO (Modèle Régional d'Océan), which is developed at Institut Maurice-Lamontagne of the Department of Fishers and Oceans Canada. This coupled model will be used to study the regional climate change around Hudson Bay region. The results show that the regional climate in Quebec is very sensible to the Hudson Bay, especially in the north of Quebec. The atmospheric temperature near surface could change greatly due to the presence of sea ice. Since the coupled model is able to reproduce the coverage of sea ice reasonably, it seems to be a reliable model to study the regional climate over Quebec.

1. Introduction

One of the most important features of Hudson Bay is the highly variable sea ice coverage. The Hudson Bay is completely covered by ice in winter and becomes ice free in September. The actual amount of ice and its distribution show large year to year variability. Due to its high albedo and its isolation properties, sea ice impacts on the regional climate near the Hudson Bay, especially to the region of northern Quebec that is located downwind of the Hudson Bay. The purpose of this study is to understand how sensitive the surface air temperature over Quebec region is with respect to ice coverage.

2. The diagram of coupled model

The Pipe technique is applied to couple MRCC and MRO. This technique allows MRCC, MRO and the Coupler to run in parallel with communications among different CUPs (Figure 1).

In each 30 minutes, the MRCC transfers screen air temperature, wind, humidity, long wave and short radiations and precipitation to MRO. At the same time, the MRO transfers sensible, latent heat fluxes, albedo, sea surface temperature, ice concentration, ice movement and sea current to MRCC. In order to have all fluxes be conserved at the coupling interface, all fluxes mentioned above are calculated in one model and then transferred to the other.

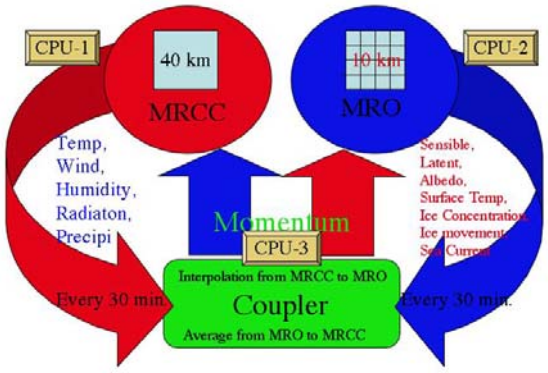

Figure 1. Diagram of coupled model

3. Results

The simulations of the coupled model begin on 1st of August 1996. In order to learn the sensitivity of ice to the regional climate in Quebec, two simulations are performed. The difference between the two simulations lies in the initialization of ocean temperature for Hudson Bay ocean model. One simulation starts with normal initialization of ocean temperature for Hudson Bay. Another starts with a warmer state of ocean temperature. The simulation starting with warmer temperature (around 3-5 C warmer) results in less ice and we might find some differences in atmosphere due to this ice difference.

Fig. 2 shows the simulated ice concentration (monthly average) for December 1996 with normal initialization of ocean temperature for Hudson Bay ocean model. Fig. 3 shows the same as Fig. 2 but with warmer initialization. Clearly in the normal simulation, the ice coverage is about 40 – 90 % in the most area of Hudson Bay, while in the warmer simulation, the ice appears only in the half of the Hudson Bay area.

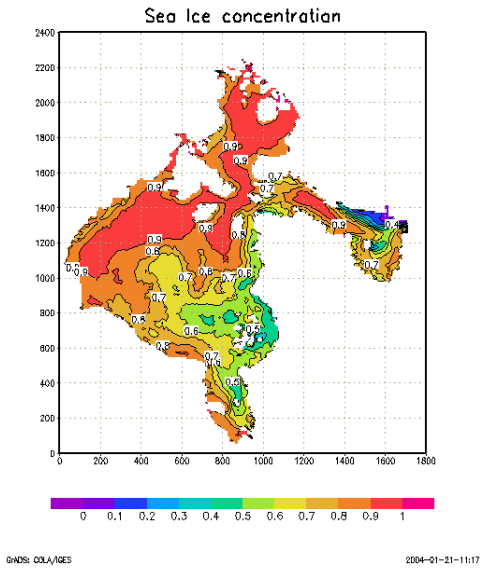

Figure 2. Simulated ice concentration in Dec. 1996 with normal initialization of ocean temperature for Hudson Bay ocean model

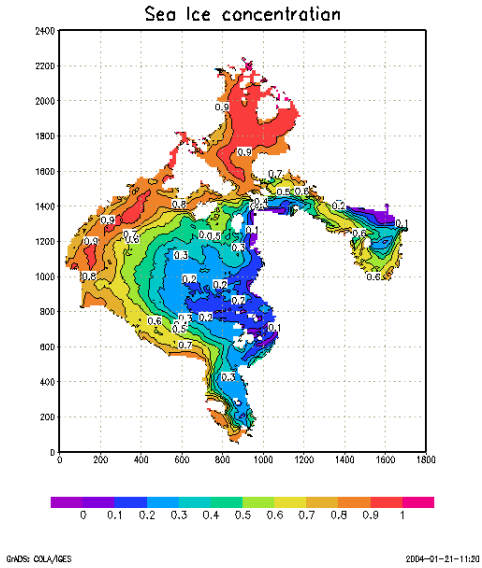

Figure 3. Simulated ice concentration in Dec. 1996 with warmer initialization of ocean temperature for Hudson Bay ocean model

This ice difference results in the difference of atmospheric temperature around Hudson Bay region. Fig. 4 represents the air temperature at 1000 mb in December 1996 from normal simulation (corresponding to Fig. 2). Fig. 5 represents the difference of air temperature between the warmer simulation and the normal simulation. The difference can reach 0.5 C to 2.0 C over the northern Quebec region.

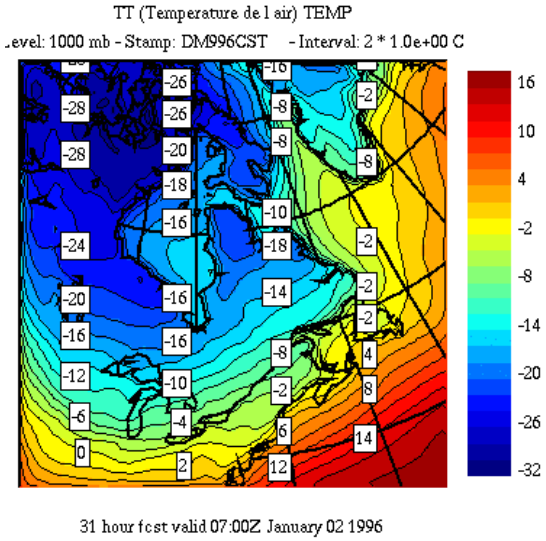

Figure 4. Simulated air temperature in Dec. 1996 (monthly mean) at 1000 mb corresponding to Fig. 2.

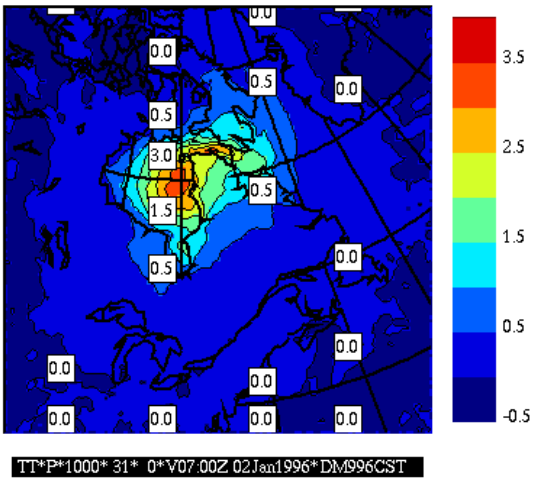

Figure 5. The difference of air temperature (monthly mean) at 1000 mb between the warmer simulation and the normal simulation (Warmer – Normal)

References

Caya, D., and R. Laprise (1999). A semi-implicit semi-Lagrangian regional climate model: The Canadian RCM. Monthly Weather Review **127**(3): 341-362.

François J. Saucier (1998). A 3D coupled ice-ocean model applied to Hudson Bay. Journal of Geophysical Research, 103, No C12, P27,689-27,705

Effects of atmospheric physical processes to the intensity of typhoons and their ocean responses

Akiyoshi Wada

Meteorological Research Institute, Tsukuba, Ibaraki, 305-0052, Japan
E-mail:awada@mri-jma.go.jp

1. Introduction

In the Japan Meteorological Agency (JMA), a typhoon model with renewal physical processes has been operated since July, 2003. In the present report, this model of which horizontal resolution was 20km around the typhoon center was coupled with a mixed layer ocean model. Numerical experiments concerning with the intensity prediction of typhoons and their ocean responses were conducted using the typhoon model and the coupled model. Conveniently, only sea surface boundary process was replaced into the old version which was based on Kondo (1975). Consequently, precipitation and radiation processes are modified from the old typhoon-ocean coupled model. Three cases are numerically experimented with two different precipitation and radiation schemes and with or without ocean coupling. Naming convection of the numerical experiments is shown in Table 1. Typhoon BILIS in August 20, 2000, Typhoon WUTIP in August 28, 2001, and Typhoon PHANFONE in August 13, 2002, which dates mean the initial time of time integration, are taken as the case study.

2. Precipitation and Radiation

In the previous typhoon model (TYMOLD), cloud water content and cloud cover were diagnostically estimated by empirical formulas. In the case of TYMKON and CMKON, cloud processes are described by prognostic equations for cloud liquid water and by diagnostic relation for precipitation. As for the mixed phase, the distinction between the water and ice phase is made as a function of temperature. At the temperature less than -15℃, the phase was assumed to be ice. At the temperature more than 0℃, the phase was assumed to be water. Cloud ice content is proportionally determined in the mixed phase between -15℃ and 0℃. In the cumulus parameterization of Arakawa and Shubert (1974), an enhanced mechanism of cumulus convection is introduced. However, a treatment of the vertical transport of horizontal momentum by convection has not been introduced. A treatment of mid-level convection would change to a mass flux scheme, which was previously treated as the moist convective adjustment. A broad-band flux emissivity method for four spectral bands is used for longwave radiation. A two-stream formulation using the delta-Eddington approximation of which spectrum is divided into 18 bands is used for shortwave scattering and absorption. In the previous shortwave model used in TYMOLD and CMOLD, planetary albedo under a clear sky was under-evaluated in comparison to the observation. Here, a scheme with Briegleb (1986) parameters is used. A direct effect of aerosol to shortwave and longwave radiation is additionally installed. A treatment of cloud fraction under a clear and cloudy sky in the shortwave radiation is also refined in TYMKON and CMKON. This enables to treat multiple reflections between layers accurately. A parameterization of an ice particle effective radius is modified. A parameterization of cloud emissivity for longwave radiation is newly formulated. Absorption coefficients of cloud water and ice represent a function of the effective radius. The cloud emissivity is estimated by formulas of Kiehl and Zender (1995) and Chin (1994).

3. Results

Differences of minimum sea level pressures (MSLPs) between TYMOLD and TYMKON and between CMOLD and CMKON are evident in Fig. 1(a)-(c) and Table 2-1. However, the issue that the amount of MSLP is under-evaluated still remains in the predictions of Typhoon BILIS and Typhoon WUTIP. In the predictions of Typhoon WUTIP and Typhoon PHANFONE, each intensity in the cases of TYMKON and CMKON is stronger than that in the cases of TYMOLD and CMOLD (Table 2-2), while this result seems not to be in accordance with that in the prediction of Typhoon BILIS (Fig.1(a)) particularly at around T+30h. Nevertheless, the intensity in the prediction of Typhoon BILIS in the cases of TYMKON and CMKON is stronger than that in the cases of TYMOLD and CMOLD in the latter integration. Modification of precipitation and radiation processes doesn't affect only the intensity prediction but also the size of typhoons. The sizes of the typhoons in the case of CMKON are respectively larger than those in the case of CMOLD (Table 3-1). This result is completely opposite to that by the ocean coupling effect (Table 3-2). In addition, the modification causes the differences of horizontal distribution of precipitation and turbulent heat fluxes. The precipitation in the cases of TYMKON and CMKON tends to concentrate on around a typhoon although that in the cases of TYMOLD and CMOLD which is covered the wider region. In fact, the modification of physical processes including prognostic the cloud water content leads

to change the distributions of cloud fraction, solar radiation and long-wave radiation. Rainfall is related to the variation of salinity near the sea surface. The decrease of sea surface temperature (SST) by turbulent mixing is comparably small due to stabilization in the upper layer caused by fresh water. Table 4 indicates maximum SST decrease of three typhoons during 72 hours in the cases of CMOLD and CMKON. In the prediction of Typhoon BILIS, maximum SST decrease is greater in the CMOLD experiment than that by a new model, while maximum SST decrease is greater in the CMKON experiment than that in the CMOLD experiment. In particular, the difference of 0.6 degree between CMOLD and CMKON is occurred in the prediction of Typhoon PHANFONE. The difference of SST decrease is concerned with the simulated intensity of the typhoons. The differences of MSLPs between TYMOLD and TYMKON are greater than that between CMOLD and CMKON (Table 2-2). In consequence, modification of the precipitation and radiation processes has less impact on the intensity of typhoon in the coupled model than that in the typhoon model.

Acknowledgements
The original codes of modified physical processes were offered by Mr. Takuya Hosomi and Mr. Ryota Sakai in JMA.

References
Arakawa and Shubert (1974): Interaction of a cumulus cloud ensemble with the large-scale environment, Part I. *J. Atmos. Sci*, **31**, 674-701.
Briegleb (1986): Comparison of Regional Clear-Sky Albedos Inferred from Satellite Observations and Model Computations, *J. Climate Appl. Meteor.*, **25**, 214-226.
Chin (1994): The impact of the ice phase and radiation on a midlatitude squall line system, *J. Atmos. Sci.*, **51**, 3320-3343.
Kiehl and Zender (1995): A prognostic ice water scheme for anvil clouds, World Climate Programme Research, WCRP-90, WMO/TD-No.713, 167-188.
Kondo (1975): Air-sea bulk transfer coefficients in diabatic conditions. *Bound. Layer Met.*, **9**, 91-112

Table1 Kinds of numerical experiments and their naming convention

	Couple	Non-couple
OLD PHYSICS	CMOLD	TYMOLD
NEW PHYSICS	CMKON	TYMKON

Table 2-1 The greatest MSLP difference between TYM and CM.

CM-TYM	BILIS(hPa)	WUTIP(hPa)	PHANFONE(hPa)
OLD	10.5	8.4	15
KON	9.4	15.9	16.3

Table 2-2 The greatest MSLP difference between OLD and KON.

OLD-KON	BILIS(hPa)	WUTIP(hPa)	PHANFONE(hPa)
TYM	10.1	14.1	11.3
CM	11.8	8.0	8.6

Table 3-1 Averaged ratio of size by the couple model with an old physical package to that by the coupled model with a new one

Couple	BILIS	WUTIP	PHANFONE
OLD/KON	1.12	1.03	1.03

Table 3-2 Averaged ratio of size by the couple model to that by the non-coupled model

CM/TYM	BILIS	WUTIP	PHANFONE
OLD	0.976	0.964	0.976
KON	0.979	0.967	0.954

Table 4 Maximum SST decrease during 72 hours by coupled models

	BILIS	WUTIP	PHANFONE
OLD	-2.14°C	-1.82°C	-2.15°C
KON	-1.71°C	-1.96°C	-2.75°C

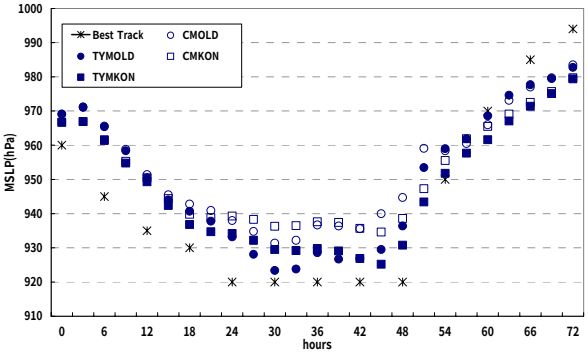

Fig.1(a) Minimum sea level pressure for Typhoon BILIS.

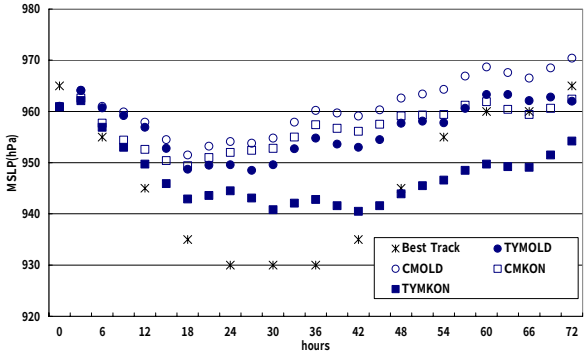

Fig.1(b) Minimum sea level pressure for Typhoon WUTIP.

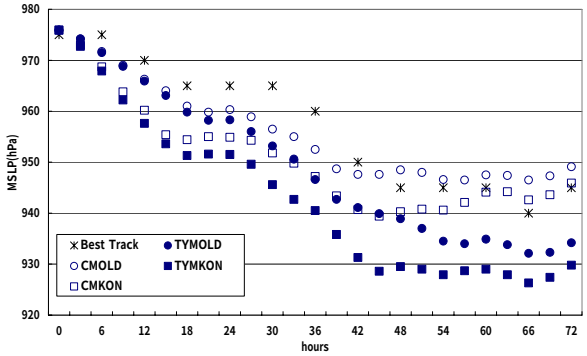

Fig.1(c) Minimum sea level pressure for Typhoon PHANFONE.

A role of surface boundary processes in a typhoon-ocean coupled model

Akiyoshi Wada

Meteorological Research Institute, Tsukuba, Ibaraki, 305-0052, Japan
E-mail:awada@mri-jma.go.jp

1. Introduction

In the numerical simulation, intensification of a simulated typhoon could be suppressed when the variation of sea surface temperature (SST) was taken account of during the passage of the typhoon. Otherwise, tuning parameters of sea surface processes, modification of sea surface roughness length, could also suppress intensification of the typhoon under the presumption of Monin-Obukhov similarity theory. The former is usually observed by ship and satellite observation. On the other hand, the latter is closely related to the ratio of the enthalpy coefficient to the drag one and remains ambiguity. Theoretical approach (Emanuel, 1995) suggested that the ratio was from 0.75 to 1.5, while observation (e.g. Fairall et al. 1996) showed that the ratio was 0.4 under windy (more than 20m/s) condition. For the purpose of investigating the identification between the ocean coupling process and the sea surface process, numerical simulations were conducted using a typhoon-ocean coupled model with two parameterizations of sea surface processes.

2. Sea surface processes

The sea surface processes in the typhoon-ocean coupled model have been based on formulas by Louis (1981), which the Monin-Obukhov similarity theory is presumed. The bulk coefficients are functions of sea surface roughness length and Richardson number, depending on wind velocity at the height of 10m. One parameterization of sea surface roughness length was derived from Kondo (1975). The formulation (1) and (2) depends on wind velocity at 10m height.

$$z_0 = -34.7\times10^{-6} + 8.28\times10^{-4}u^* \qquad u_{10} \le 25(m/s) \tag{1}$$

$$z_0 = -0.227\times10^{-2} + 3.39\times10^{-3}u^* \qquad u_{10} > 25(m/s) \tag{2}$$

These lengths are used as z_{0m} for momentum and z_{0h} for turbulent heat. The other approach that (3) in Beljaars (1995) is used for momentum and (4) in Garratt (1992) is used for turbulent heat.

$$z_{0m} = \frac{0.11\nu}{u^*} + \frac{\alpha}{g}u^{*2} \tag{3}$$

$$z_{0h} = \exp\left\{-2.48\times\left(\frac{u^* z_{om}}{\nu}\right)^{0.25} + 2.0\right\} \tag{4}$$

Four kinds of simulations were conducted taking account of whether ocean coupling was including or not, and the parameterization of sea surface roughness length was that of Kondo 1975) or Beljaars(1995) and Garratt (1992). Detail information for experiments is summarized in Table 1. Typhoon BILIS in August 20, 2000, Typhoon WUTIP in August 28, 2001, and Typhoon PHANFONE in August 13, 2002, which dates respectively mean the initial time of time integration, are selected as the case study.

3. Results

Results of minimum sea level pressure (MSLP) in the predictions of three typhoons are respectively shown in Fig. 1(a)-(c). The MSLPs of CMJMA and CMKON are higher than those of TYMJMA and TYMKON. The greatest difference of MSLP between TYMJMA and CMJMA is from 8.8hPa of Typhoon BILIS to 11.9hPa of Typhoon WUTIP (Table 2-1), while that of MSLP between TYMKON and CMKON is from 9.4hPa of Typhoon BILIS to 16.3hPa of Typhoon PHANFONE (Table 2-2). Thus, the greatest difference of MSLPs between TYMKON and CMKON is higher than that between TYMJMA and CMJMA. The result is particularly prominent in the predictions of Typhoon WUTIP and Typhoon PHANFONE. By comparing the result shown in Table 2-1 with that shown in Table 2-2, the ocean coupling effect is more significant in the MSLP prediction than the effect of sea surface roughness length concerning. This result concerning with the intensity predictions is closely related to the size of the typhoon. A radius of 15m/s wind velocity is defined as an index shown in the size of a typhoon. The ratio of size by four experiments is shown in Table 3-1 and Table 3-2. The ocean coupling effect causes the reduction of the size, while the size in the CMKON experiment is larger than that in the CMJMA experiment except Typhoon BILIS. The result is opposite to the MSLP prediction. The ratio is so large in the predictions of Typhoon WUTIP and Typhoon PHANFONE that the effect of parameterization of sea surface roughness length is greater than that by ocean coupling in turn. Because the size of typhoons is considered to have a large influence on the track of typhoons, the effect of parameterization of sea surface

roughness may affect the track of Typhoon WUTIP and Typhoon PHANFONE more than that by ocean coupling. The intensity and the size of typhoons have a great impact on cooling of the sea surface through the air-sea interaction. The air-sea interaction depends on the ratio of enthalpy coefficients to drag coefficients. According to Bao et al. (2002), the ratio of enthalpy coefficient to drag coefficient was less than 0.7 under windy (more than 20m/s wind velocity) conditions. The difference of cooling of the sea surface (Table 4) may be related to the ratio. In this study, the ratios of TYMJMA and CMJMA tend to be smaller than those of TYMKON and CMKON.

Acknowledgements
The original codes of modified physical processes were offered by Mr. Takuya Hosomi and Mr. Ryota Sakai in JMA.

References
Bao et al. (2002): Sensitivity of numerical simulations to parameterizations of roughness for serface heat fluxes at high winds over the sea. *Mon. Wea. Rev.* **130**, 1926-1932.
Beljaars (1995): The parameterization of surface fluxes in large-scale models under free convection. *Quart. J. Roy. Meteor. Soc.*, **121**, 255-270.
Emanuel (1995): Sensitivity of tropical cyclones to surface exchange coefficients and a revised steady-state model incorporating eye dynamics. *J. Atmos. Sci.*, **52**, 3969-3976.
Fairall et al. (1996):Bulk parameterization of air-sea fluxes for tropical ocean global atmosphere coupled-ocean atmosphere response experiment. *J. Geophys. Res.*, **101**, 3747-3764.
Garratt (1992): The atmosphere boundary layer. Cambridge University Press, 316pp.
Kondo (1975): Air-sea bulk transfer coefficients in diabatic conditions. *Bound. Layer Met.*, **9**, 91-112.
Louis et al. (1981): A short history of the operational PBL-parameterization at ECMWF, Workshop on Planetary Boundary Layer Parameterization 25-27 Nov. 1981, 59-79.

Table 1 Kinds of numerical experiments and their naming convention

Experiments	Coupling?	Roughness Length
TYMJMA	No	Beljaars and Garratt
CMJMA	Yes	Beljaars and Garratt
TYMKON	No	Kondo
CMKON	Yes	Kondo

Table 2-1 The greatest MSLP difference between TYM and CM.

CM-TYM	BILIS(hPa)	WUTIP(hPa)	PHANFONE(hPa)
JMA	8.8	11.9	11
KON	9.4	15.9	16.3

Table 2-2 The greatest MSLP difference between JMA and KON.

JMA-KON	BILIS(hPa)	WUTIP(hPa)	PHANFONE(hPa)
TYM	6.2	10.5	15.9
CM	6.8	6.4	9.8

Table 3-1 Averaged ratio of size by the couple model to that by the non-coupled model

CM/TYM	BILIS	WUTIP	PHANFONE
JMA	0.979	0.959	0.955
KON	0.979	0.967	0.954

Table 3-2 Averaged ratio of size by Kondo to that by Beljaars and Garratt

Couple	BILIS	WUTIP	PHANFONE
KON/JMA	0.99	1.07	1.05

Table 4 Maximum SST decrease during 72 hours by coupled models

	BILIS	WUTIP	PHANFONE
JMA	-2.30℃	-1.98℃	-2.48℃
KON	-1.71℃	-1.96℃	-2.75℃

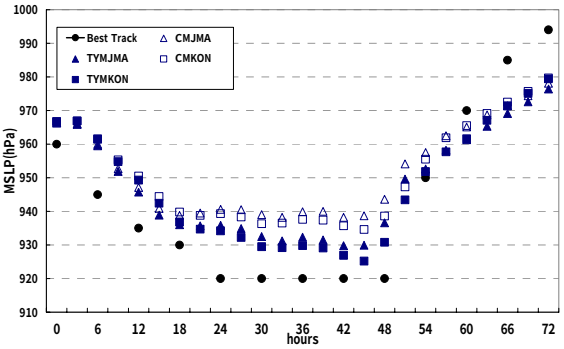

Fig.1(a) Minimum sea level pressure for Typhoon BILIS.

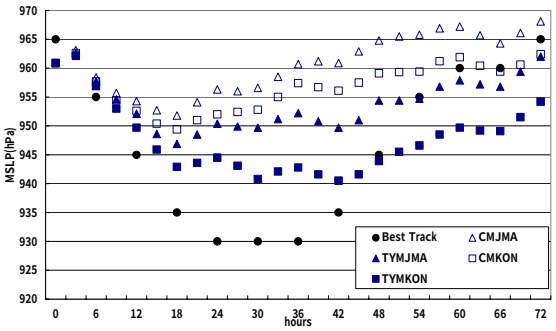

Fig.1(b) Minimum sea level pressure for Typhoon WUTIP.

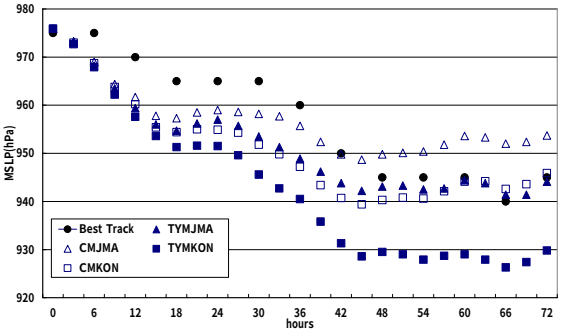

Fig.1(c) Minimum sea level pressure for Typhoon PHANFONE.

Development of a coupled regional climate model for the Arctic

Klaus Wyser, Ralf Döscher, H.E.Markus Meier, Colin Jones
Rossby Centre, SMHI, 601 76 Norrköping, SWEDEN

Background

Recent observations and climate modelling results (Cubasch et al 2001, Serreze et al 2000) have highlighted the Arctic region as particularly vulnerable to potential anthropogenic climate change. Global model projections of the future climate show the largest surface warming over sea ice covered regions of the Arctic Ocean, where an initial climate warming is hypothesised to lead to sea ice melt, a reduction in the surface albedo and further melting and warming through increased absorption of solar radiation (i.e positive feedback). However, Global Climate Model simulations of the Arctic vary widely in quality and many of the key physical processes that must be parameterised are poorly understood.

One of the main objectives of the EU-sponsored GLIMPSE project (http://www.awi-potsdam.de/www-pot/atmo/glimpse/index.html) is to improve the description of physical processes in the Arctic and to develop parameterisations that can be used in climate models. As a contribution to GLIMPSE, the Rossby Centre at SMHI develops a coupled regional climate model for the Arctic based on the existing RCAO model (Döscher et al 2002) that combines the atmosphere model RCA (Rummukainen et al 2001) and the ocean model RCO (Meier et al 2003). The coupled model has been developed for mid-latitudes and therefore requires some adjustments for the relocation to the Arctic. Sea-ice and snow are important components of the Arctic climate – especially with regard to their role for the feedback with radiation – and the correct description of the melting, freezing and transport will be crucial for the coupled model and require special attention when setting up the model. Clouds are another important issue for the Arctic climate and we will study the interaction between clouds, radiation, and the underlying sea-ice to understand the complex dynamics and feedback between the various components.

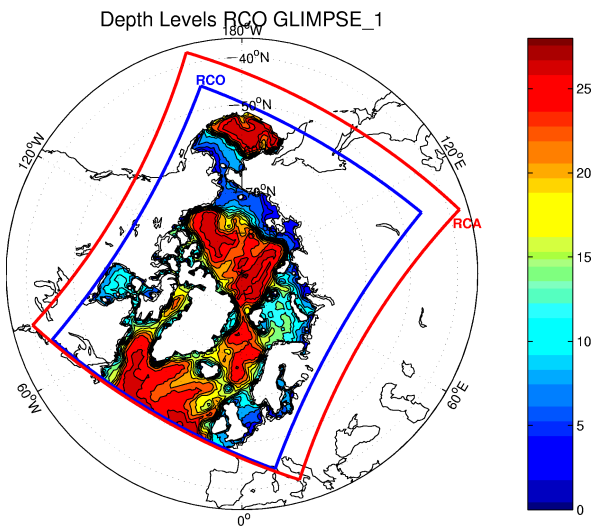

Figure 1 Setup of ocean (blue) and atmosphere (red) model domain for GLIMPSE. Color scale denotes depth for ocean model

Model setup

The setup of our coupled regional climate model for the Arctic is shown in Figure 1. The ocean model covers the central Arctic Ocean and the North Atlantic north of 50N. The Bering Sea is also included in order to realistically simulate the inflow variability through the Bering Strait. The horizontal resolution is 0.5 degrees or approximately 50 km in a rotated coordinate system centred over the North Pole. At the lateral boundaries sponge zones with relaxation to climatology are utilized. It is planned to replace these sponge zones with active open boundary conditions. The ocean model is coupled with a Hibler-type two-level (open water and ice) dynamic-thermodynamic sea ice model. The sea ice model utilizes the same horizontal grid as the ocean model.

The atmosphere model covers the same area as the ocean model and additionally some of the surrounding landmasses. The atmosphere and ocean model share the same horizontal grid in the common area. The present model configuration consists of 24 vertical levels but an increase to 31 levels is planned. At the boundaries, the atmosphere model is driven with 6-hourly ERA-40 fields.

The ocean and atmosphere models are coupled through the OASIS coupler that handles all data communication and – if necessary – interpolations between atmosphere and ocean grids (Terray et al. 1999). Ocean and atmosphere model time step are 10 and 30 minutes, respectively, and the coupling time step is 3 hours.

First results

First simulations with the atmopshere model alone have been performed to test the setup. As an example we show one year of monthly mean sea-level pressure over the central Arctic (north of 75N) from two runs compared to the observational ECMWF analyis (Fig. 2). The two model simulations differ in their description of the sea-ice, GL_OBS_ICE uses the sea-ice field from the ERA-40 analysis (derived from SSM/I observations) while GL_CLIM_ICE uses a climatological sea-ice field. None of the simulations shows a systematic bias. Neither simulation matches the observation in every month; sometimes GL_OBS_ICE is in better agreement and sometimes GL_CLIM_ICE. The difference between the two model simulations is of the same order as the difference between any of the simulations and the ECMWF analysis.

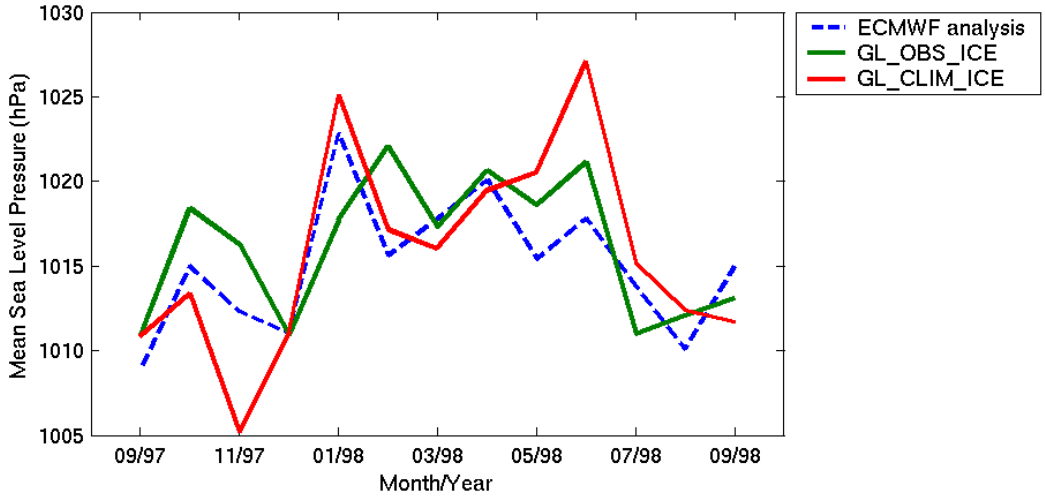

Figure 2 Monthly mean se level pressure in thecentral Arctic for 2 simulations (described in text) and ECMWF operational analaysis.

The example emphasises the role of the sea-ice for the variability of the Arctic climate. Future simulations with the coupled ocean-atmosphere model will include an interactive sea-ice description that will allow us to study the variability of the Arctic climate under consideration of the feedback between sea-ice and circulation.

References

Cubasch U, G.A.Meehl, G.J.Boer, R.J.Stouffer, M.Dix, A.Noda, C.A.Senior, S.Raper and K.S.Yap (2001). Projections of Future Climate Change. In *Climate Change 2001: The scientific basis. Contribution of Working Group 1 to the Third Assessment Report of the Intergovernmental Panel on Climate Change*. Cambridge University Press, 881pp.

Döscher R., U.Willén, C.Jones, A.Rutgersson, H.E.M.Meier, U.Hansson and L.P.Graham (2002). The development of the regional coupled ocean-atmosphere model RCAO. *Boreal Env. Res. 7*, 183-192.

Meier, H.E.M., R. Döscher, and T. Faxen (2003). A multiprocessor coupled ice-ocean model for the Baltic Sea: Application to salt inflow. *J. Geophys. Res. 108(C8)*, 3273.

Rummukainen M, J.Räisänen, B.Bringfelt, A.Ullerstig, A.Omstedy, U.Willén, U.Hansson and C. Jones (2001). A regional climate model for northern Europe: model description and results from the downscaling of twp GCM control simulations. *Clim. Dyn. 17*, 339-359.

Serreze M.C. and co-authors 2000. Observational evidence of recent changes in the northern high-latitude environment. *Climatic Change 46*, 159-20.

Terray L., S.Valcke and A.Piacentini (1999). *OASIS 2.3 Ocean Atmosphere Sea Ice Soil users guide*. CERFACS TR/CGMC/99-37, 82 pp.

Upgrade of JMA El Niño Forecast Model (JMA-CGCM02)

Goro Yamanaka, Yoshinobu Nikaidou, Masayoshi Ishii, and Yoshiteru Kitamura
yamanaka@met.kishou.go.jp
Japan Meteorological Agency, Tokyo, JAPAN

1. Introduction

The Japan Meteorological Agency (JMA) has operated a Coupled ocean-atmosphere General Circulation Model (JMA-CGCM01) for the prediction of ENSO since 1999. In July 2003, JMA put into operation a new coupled model (JMA-CGCM02). This model revised the physical process in the Atmosphere General Circulation Model (AGCM) and introduced a new Ocean Data Assimilation System (ODAS). The ENSO forecast of JMA-CGCM02 show better performance. The improvement is more evident within shorter lead time until 7 to 8 months. This article describes the changes of specification of the new model and the forecast skill.

2. Outline of JMA-CGCM02

Major specifications and their change from the former model are summarized in Table 1.

JMA-CGCM02 includes the following main three changes:

(1) The atmospheric part is a lower resolution version (T42L40) of the current three-month prediction model in operation since March 2001. Compared with the former AGCM, the top level height is increased and the vertical resolution is enhanced. The cumulus convection and radiation schemes are revised. Cloud water content becomes a prognostic variable.

(2) The oceanic part is a Bryan-Cox type ocean general circulation model (OGCM) and is identical to the former OGCM only except slight change in the vertical mixing parameterization. In a new ODAS, a three dimensional variational analysis scheme based on Derber and Rosati (1989) is introduced. The nudging scheme is replaced by an incremental analysis update scheme (Bloom et al., 1996). Salinity and sea surface height data are newly assimilated in addition to temperature.

(3) The flux adjustment amounts of momentum and heat flux are newly derived with the observed SST variations.

The coupling takes place every 24 hours, that is, the ocean model gives the sea surface temperature to the atmospheric model, and the atmospheric model provides the daily mean heat and momentum flux to the ocean model. The fresh water flux is not given in the forecast integration.

Table 1: Major specifications of JMA-CGCM02 and their change from the former model

Atmospheric General Circulation Model

	Former model (T42L21 GSM8911)	New Model (T42L40 GSM0103)
Vertical resolution	21 levels (model top: 10hPa)	40 levels (model top: 0.4hPa)
Cumulus convection parameterization	Kuo scheme	Prognostic Arakawa-Schubert scheme
Cloud water content	Diagnostic	Prognostic variable
Radiation process	Solar, Infrared	Solar, Infrared, direct aerosol effect

Ocean Data Assimilation System
(OGCM : 2.5° (lon.) x 0.5 - 2° (lat.), L20)

	Former model	New Model
Analysis scheme	Two-dimensional optimum interpolation method	Three-dimensional variational method
Assimilation scheme	Nudging	Incremental Analysis Update
Assimilated data	Temperature	Temperature, Salinity, Sea surface height
Analysis interval	5-day	1-day

3. Predictions of SST variability by JMA-CGCM02

Prediction skill for the tropical Pacific SST anomalies is estimated through evaluation of 1-year hindcast experiments (a set of 117 runs) initiated monthly from January 1988 to September 2002.

Figure 1 shows anomaly correlation coefficient (ACC) and root mean square error (RMSE) for the Nino-3.4 (5S-5N, 170W-120W) SST anomalies. As of ACC, the model prediction skill is higher than the persistence prediction skill at 3-month or longer lead time. The ACC of the model is about 0.7 at 6-month lead time. As of RMSE, the skill of the model exceeds that of the persistence prediction after 5-month lead time, and is better than that of the climatology prediction until 9-month lead time. However, comparison of the skill for summer and winter (not shown) indicates that, even with this model, the skill levels for the summer predictions are still lower than those for the winter predictions, suggesting the "spring prediction barrier".

Figure 2 shows the spatial distributions of two-season-lead predicted versus observed SST anomaly temporal correlations for JMA-CGCM02 and for the persistence forecasts. The skill of the model is higher than the persistence prediction over most of the tropical Pacific at 6-month lead time. The highest skill is found especially in the eastern equatorial Pacific around 150W, where SST variability associated with ENSO is large. In the western tropical Pacific and the Indian Ocean, some promising skill can be found, though the values of the ACC are relatively small.

References

Bloom, S. C., L. L. Tacks, A. M. daSilva, and D. Ledvina, 1996: Data assimilation using incremental analysis updates. *Mon. Wea. Rev.*, 124, 1256-1271.

Derber, J. C. and A. Rosati, 1989: A global oceanic data assimilation technique. *J. Phys. Oceanogr.*, 19, 1333-1347.

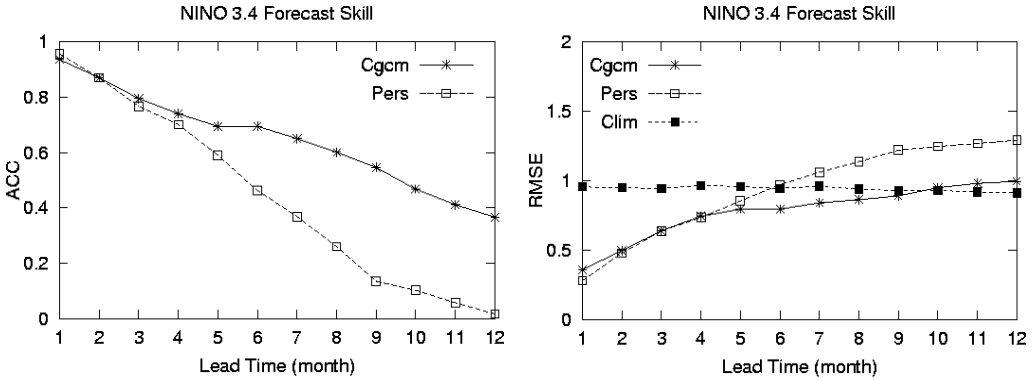

Figure 1: Anomaly correlation coefficient (ACC) (left) and root mean square error (RMSE) (right) for the Nino-3.4 SST anomalies between prediction and observations for the period of February 1988-August 2003. The ACC and RMSE for the persistence forecasts (Pers) and RMSE for the climatology forecasts (Clim) are also shown for reference.

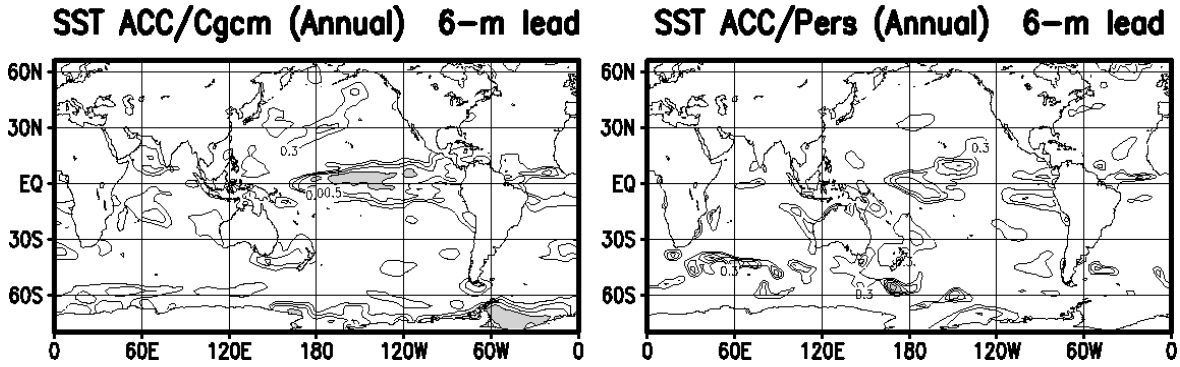

Figure 2: Temporal SST anomaly correlation coefficients with 6-month lead time for JMA-CGCM02 (left) and the persistence forecast (right). Contours are drawn only for areas where the anomaly correlation coefficients are greater than 0.3 and contour interval is 0.1. Shaded areas denote where the anomaly correlation coefficients are greater than 0.6.